ANL/MSD/CP--86957
CONF-951155--121

# IN-SITU HVEM STUDIES OF RADIATION-INDUCED SEGREGATION IN Ni-Al ALLOYS DURING SIMULTANEOUS IRRADIATION WITH ELECTRONS AND IONS

M. J. Giacobbe [a,b], N. Q. Lam [a], P. R. Okamoto [a], and J. F. Stubbins [b]
[a] Argonne National Laboratory
Materials Science Division
Argonne, IL 60439

[b] University of Illinois
Department of Nuclear Engineering
Urbana, IL 61801

May 1996



Manuscript presented at Materials Research Society Fall Meeting, Boston, MA, November 27 - December 1, 1995.

*Work supported by the U.S. Department of Energy, Basic Energy Sciences-Materials Sciences, under contract No. W-31-109-Eng-38.

# IN-SITU HVEM STUDIES OF RADIATION-INDUCED SEGREGATION IN Ni-Al ALLOYS DURING SIMULTANEOUS IRRADIATION WITH ELECTRONS AND IONS

M. J. Giacobbe [a,b], N.Q. Lam [a], P.R. Okamoto [a], J.F. Stubbins [b]
[a] Argonne National Laboratory, Materials Science Division, Argonne, IL
[b] University of Illinois at Urbana-Champaign, Department of Nuclear Engineering, Urbana, IL

## ABSTRACT

The effects of 75-keV $Ne^+$ and 300-keV $Ni^+$ bombardment on electron radiation-induced segregation (RIS) in a Ni-9at.%Al alloy were investigated in-situ using the HVEM (high voltage electron microscope)/Tandem accelerator facility at Argonne National Laboratory. The radial component of defect fluxes generated by a highly-focused 900-keV electron beam was used to induce segregation of Al atoms towards the center of the electron irradiated area via the inverse-Kirkendall effect. The radial segregation rate was monitored by measuring the increase in the diameter of the Al enriched zone within which $\gamma'$-$Ni_3Al$ precipitates form during irradiation. Both dual electron-ion and pre-implanted ion-electron irradiations were performed in an attempt to separate the contributions of energetic displacement cascades and implanted ions acting as defect trapping sites to RIS suppression. It was found that 75-keV $Ne^+$ implantation has a retarding effect on RIS.

## INTRODUCTION

Radiation-induced segregation (RIS) of the chemical constituents of an alloy is a well-known phenomenon that occurs because defect annihilation at sinks induce defect fluxes that tend to couple preferentially to atom fluxes of a particular alloy component [1,2]. The preferential coupling can arise via the inverse-Kirkendall effect or via defect-solute interactions that result in the formation of mobile solute-defect complexes [1-3]. RIS processes driven by radial gradients in the concentration of point defects generated by highly-focused electron beams have been used to induce precipitation of $\gamma'$-$Ni_3Al$ and $\gamma'$-$Ni_3Si$ phases in undersaturated Ni-Al and Ni-Si solid-solutions respectively, and to cause a redistribution of these phases in initially two phase alloys [4-7]. As shown by Lam and Okamoto [5-8], the redistribution of the $\gamma'$-phase provides a direct measure of electron beam-induced solute segregation rate. In the present work, we show that the electron beam driven segregation rate in a Ni-9at.%Al alloy can be altered by irradiating the sample simultaneously with ions or by pre-implanting the sample with ions prior to electron irradiation.

## EXPERIMENTAL PROCEDURE

In-situ electron-ion dual irradiations were carried out at the Argonne HVEM/Tandem accelerator facility. All irradiations were performed at 550°C with 900-keV electrons and either 75-keV $Ne^+$ or 300 keV $Ni^+$ ions. Ne was selected to study the effect of implanted gas atoms on segregation kinetics, while Ni was chosen to study the effect of cascade damage. TRIM calculations indicated the 99% of the 300-keV $Ni^+$ ions and 100% of the 75-keV $Ne^+$ ions are stopped within a distance of 180 nm from the top foil surface.

The defect distribution produced in a thin film by a focused electron beam is shown schematically in Fig. 1. Here $D_o$ is effective beam diameter defined by $I_T = I_o (\pi D_o/2)^2$ where $I_T$ is the total electron current and $I_o$ is the maximum electron flux. For a Gaussian beam Do is $2\sqrt{2}\sigma$ where $\sigma$ is the standard deviation of the beam intensity profile. Previous work [5,8] on Ni-Al alloys showed that Al atoms diffuse uphill against the flow of vacancies and that the irradiated area where the defect concentration profile is concave downward becomes enriched with Al. The enrichment continues until the Al solubility limit is reached at which point the $\gamma'$-$Ni_3Al$ phase can nucleate and grow [9]. The diameter of the zone of precipitation sharply defines the Al-enriched region, and its growth rate provides a direct measure of the radial segregation rate.

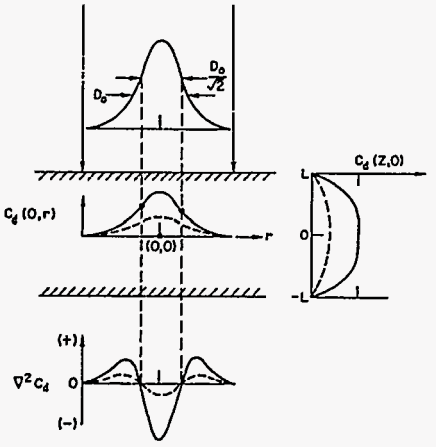


Figure 1. Top to bottom: electron beam profile, radial and axial defect production profile, and radial defect divergence. The defect gradients determine the direction and magnitude of the defect flux, while the defect divergence determines the local rate of solute accumulation or depletion [6-8].

Peak electron damage rates employed in the present study varied between 7.2-9.9x$10^{-4}$ dpa/s. For the ion bombardments, peak damage rates were 5.5x$10^{-5}$ and 2.4x$10^{-4}$ for $Ne^+$ and $Ni^+$ ions respectively. Three types of irradiations were performed: (i) electrons only, (ii) dual irradiations with electrons and ions, and (iii) ion implantation followed by electron irradiation. To provide reference markers during (ii) and (iii), small zones of the $\gamma'$-$Ni_3Al$ phase were pre-formed with electrons. In all cases the shape of the focused electron beam and hence that of the precipitation zone was elliptical. The beam intensity was assumed to be bi-Gaussian and of the form $I(x,y) = I_o\exp\{-(x/a_o)^2 - (y/b_o)^2\}$ where $a_o = \sqrt{2}\sigma_a$ and $b_O = \sqrt{2}\sigma_b$ ($\sigma$'s are the standard deviation of the beam profile along the major and minor axes). The dimensions of the precipitate zones along their major and minor axes were taken as $a/a_o$ and $b/b_o$ respectively. Normalizing measurements with respect to beam dimensions allows both $a/a_o$ and $b/b_o$ to be shown on the same scale.

## RESULTS

Results are summarized in Figures 2, 3, 4, and 5. Figures 2 and 3 show the $\gamma'$ growth under electron only, dual electron-ion, and electron only after ion implantation irradiation conditions. In both the dual and pre-implanted cases, a $\gamma'$ zone was seeded with a 900-keV electron irradiation before the samples were subjected to any ion bombardment as seen in Figures 4b-c, t = 720 s, and 5b, t = 420 s. In all cases, the focused electron beam, slightly elliptical in geometry, ranges from 1.0-1.2 μm on the major axis and 0.80-0.95 μm on the minor axis (the beam dimensions are $a_o$ and $b_o$, defined in the previous section). All beam dimension calculations are dependent on the assumption that the electron beam is bi-Gaussian in nature.

The effects of 75-keV $Ne^+$ implantation on RIS are demonstrated in Figure 2. During the dual electron-ion irradiation, the growth of the precipitate zone was somewhat suppressed (micrographs in Figure 4b). After ion implantation to $10^{15}$ ion/cm$^2$, the growth of the precipitate zone experienced greater suppression than during dual irradiation (micrographs in Figure 4c). The effects of 300-keV $Ni^+$ on RIS are shown in Figure 3. During both dual (micrographs in Figure 5b) and pre-implanted runs, no significant difference was observed in the growth of the irradiation-induced precipitate. An interesting feature in Figures 4c and 5b is the sink free

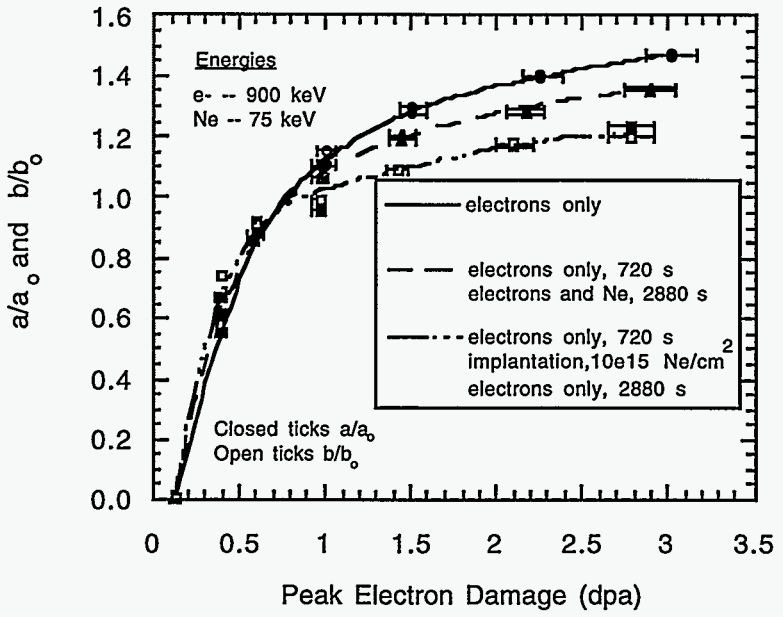


Figure 2. $\gamma'$-$Ni_3Al$ growth curve for 900-keV electron, dual 900-keV electron/75-keV $Ne^+$ ion, and pre-implanted 75-keV $Ne^+$ ion/900-keV electron irradiations at 550°C. The y-axis is the ratio of the precipitate zone size to the elliptical Gaussian beam dimensions, which allows for the normalization of irradiations with different electron beam conditions.

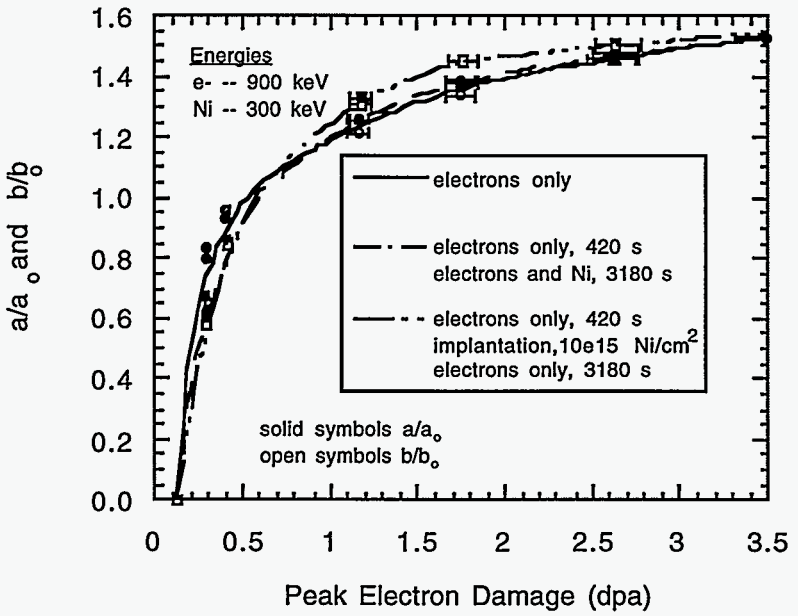


Figure 3. $\gamma'$-$Ni_3Al$ growth curve for 900-keV electron, dual 900-keV electron/300-keV $Ni^+$ ion, and pre-implanted 300-keV $Ni^+$ ion/900-keV electron irradiations at 550°C. The y-axis is the ratio of the precipitate zone size to the elliptical Gaussian beam dimensions, which allows for the normalization of irradiations with different electron beam conditions.

denuded zone surrounding the γ' precipitate zone. When $10^{15}$ ion/cm$^2$ of 300-keV Ni$^+$ were implanted, this denuded zone was replaced by a complex dislocation network.

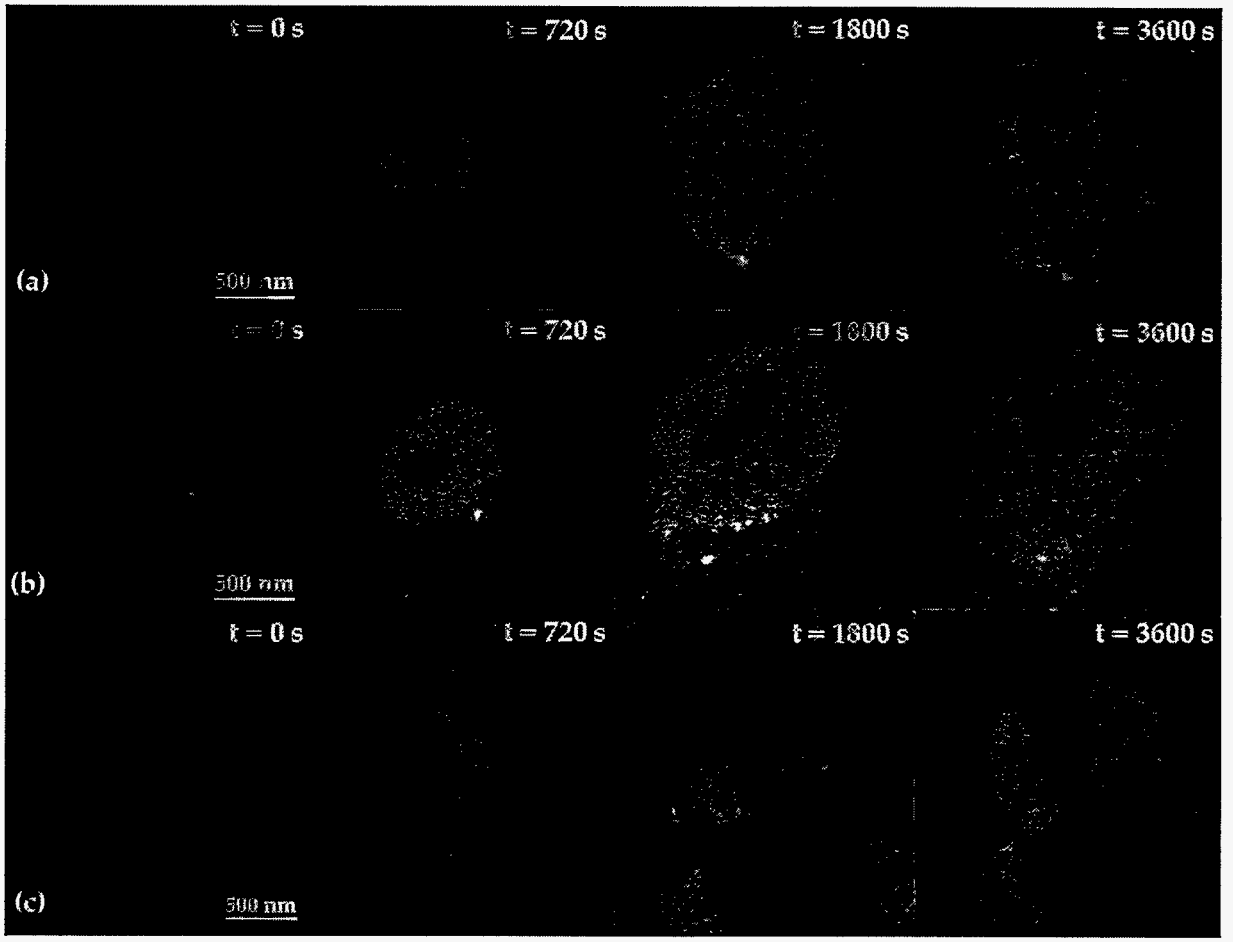


Figure 4. Precipitate growth as a function of time for (a) 900-keV electron only for 36000 s (3.02 dpa, $K_{peak} = 8.4x10^{-4}$ dpa/s), (b) 900-keV electron irradiation for 720 s (0.583 dpa) to grow the precipitate ($K_{peak} = 8.1x10^{-4}$ dpa/s) followed by dual 900-keV electron/75-keV $Ne^+$ irradiation for 2880 s (2.33 dpa), and (c) 900-keV electrons only for 720 s (0.598 dpa) to grow the precipitate ($K_{peak} = 8.3x10^{-4}$ dpa/s), followed by $10^{15}$ Ne/cm$^2$, followed by 900-keV electrons ($K_{peak} = 7.6x10^{-4}$ dpa/s) for 2880 s (2.19 dpa). All irradiations were conducted at 550°C and listed damages are from electrons only.

## DISCUSSION

Our results demonstrate that 75-keV Ne+ irradiation has a suppressing effect on RIS and that 300-keV Ni+ does not. In both cases, a sink structure develops: thus, this effect cannot be attributed to difference in the visible sink structure.

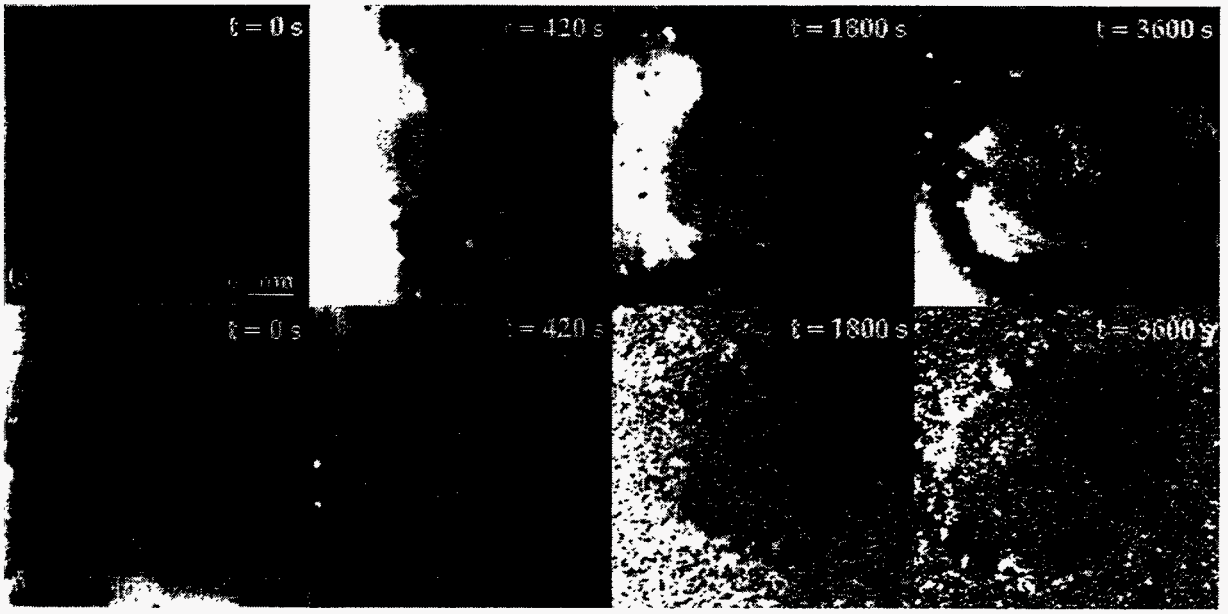


Figure 5. Precipitate growth as a function of time for (a) 900-keV electron only irradiation for 3600 s (3.49 dpa, $K_{peak} = 9.7x10^{-4}$ dpa/s) and (b) 900-keV electron irradiation for 420 s (0.407 dpa) to grow the precipitate ($K_{peak} = 9.7x10^{-4}$ dpa/s), followed by dual 900-keV electron/300-keV $Ni^+$ dual irradiation for 3180 s (3.08 dpa). All irradiations were conducted at 550oC and listed damages are from electrons only.

Since RIS is cause by the defects which survive recombination, these results suggest that the presence of Ne causes a retardation in RIS by acting as a strong vacancy trapping site, hence enhancing recombination. It has been previously suggested that He clusters can act as defect trapping sites, enhancing recombination and reducing segregation in Ni-based alloys [10]. The 300-keV $Ni^+$ ion bombardment results in the present work contradict to some extent recent dual irradiation studies of RIS in Cu-1at.%Au [11,12]. In that work, Iwase et. al [11,12] concluded the cascade remnants of energetic displacement cascades were responsible for suppressing RIS. Further investigations are necessary to clearly determine the roles of cascade remnants and defect trapping in changing RIS behavior.

As mentioned in the previous section, a sink free denuded zone is present at the periphery of the central precipitate. At the present time, the reason for the formation of this denuded zone is unknown, and further studies are necessary to determine its nature.

## CONCLUSION

In Ni-9at.%Al irradiated with 900 keV electrons at 550°C, Ne implanted at 75-keV had a suppressing effect on RIS of Al, as demonstrated by the retarded growth of the $\gamma'$-$Ni_3Al$ precipitate zone. 300-keV $Ni^+$ bombardment, however, had no effect on segregation kinetics both during dual electron-ion and pre-implantation (with $10^{15}$ Ni/cm$^2$) electron runs. These results lead to the conclusion that Ne has a suppressing effect on RIS in Ni-9at%Al.

ACKNOWLEDGMENTS

The authors would like to thank L.E. Rehn for helpful discussions, and B. Kestel, E. Ryan, S. Ockers, and L. Funk for their experimental assistance.

REFERENCES

[1] P.R. Okamoto and L.E. Rehn, J. Nucl. Mater. **83** , 2(1979).
[2] H. Wiedersich and N.Q. Lam, in: *Phase Transformations during Irradiation*, ed. F.V. Nolfi, Jr. (Applied Science Publishers, London, 1983) p. 1.
[3] R.A. Johnson and N.Q. Lam, Phys. Rev **B13**, 4364 (1976).
[4] P.R. Okamoto and H. Wiedersich, J. Nucl. Mater. **53**, 336 (1974).
[5] N.Q. Lam and P.R. Okamoto, in *Effect of Radiation on Materials: Twelfth International Symposium*, ASTM STP 870, eds. F.A. Garner and J.S. Perrin (ASTM, Philadelphia 1985) p. 430.
[6] N.Q. Lam and P.R. Okamoto, J. Nucl. Mater. **133-134**, 430 (1985).
[7] N.Q. Lam and P.R. Okamoto in *Solute-Defect Interaction: Theory and Experiment*, eds. S. Saimoto et al. (Pergamon Press, Toronto, 1986) p. 307.
[8] P.R. Okamoto and N.Q. Lam, Mat. Res. Soc. Symp. Proc. **41**, 241 (1985): N.Q. Lam, P.R. Okamoto, and G.K. Leaf, Mat. Res. Soc. Symp. Proc. **74**, 523 (1987).
[9] N.Q. Lam, G.K. Leaf, and M. Minkoff, J. Nucl. Mater. **118**, 248 (1983).
[10] T. Ezawa, E. Wakai, T. Tanabe, and R. Oshima, J. Nucl. Mater **191-194,** 1346 (1992).
[11] A. Iwase, L.E. Rehn, P.M. Baldo, and L. Funk, Appl. Phys. Lett. **67**, 229 (1995).
[12] A. Iwase, L.E. Rehn, P.M. Baldo, P.R. Okamoto, H. Wiedersich, and L. Funk, Mat. Res. Soc. Symp. Proc. **316**, 241 (1993)